

Calibration and standards beamline 6.3.2 at the Advanced Light Source

J.H. Underwood, E.M. Gullikson, M. Koike, P.J. Batson, P.E. Denham, K.D. Franck, R.E. Tackaberry and W.F. Steele
Center for X-ray Optics, Lawrence Berkeley Laboratory, University of California, Berkeley, CA 94720

(Presented on 20 October 1995)

This bending magnet beamline has been in operation since February 1995 for the characterization of optical elements (mirrors, gratings, multilayers, detectors, etc.) in the energy range 50-1000 eV. Although it was designed primarily for precision reflectometry of multilayer reflecting optics for EUV projection lithography, it has capabilities for a wide range of measurements. The optics consist of a monochromator, a reflectometer, and refocusing mirrors to provide a small spot on the sample. The monochromator is a very compact, entrance-slitless, varied-line-spacing plane-grating design in which the mechanically ruled grating operates in the converging light from a spherical mirror working at high demagnification. Aberrations of the mirror are corrected by the line spacing variation, so that the spectral resolving power $\lambda/\Delta\lambda$ is limited by the ALS source size to about 7000. Wavelength is scanned by simple rotation of the grating with a fixed exit slit. The reflectometer has the capability of positioning the sample to within 10 μm and setting its angular position to 0.002°. LABVIEW™ based software provides a convenient interface to the user. The reflectometer is separated from the beamline by a differential pump and can be pumped down in 1/2 hour. Auxiliary experimental stations can be mounted behind the reflectometer. Results are shown that demonstrate the performance and operational convenience of the beamline. © 1996 American Institute of Physics.

I. NEED FOR CALIBRATION AND STANDARDS

More sophisticated optics for the x-ray, soft x-ray and far ultraviolet spectral regions are continuously being developed for synchrotron radiation research, for astronomy, x-ray lithography, plasma research, fusion applications and many others. These developments bring with them a need for accurate calibration and standards facilities, in particular for measuring reflectivity of mirrors and multilayer coatings, transmission of thin films, bandpass of multilayers, efficiency of gratings or detectors, etc. While much can be accomplished with conventional sources and laser-produced plasmas,¹ the availability of third-generation synchrotron radiation sources and advanced optical designs, in particular for monochromators, together present opportunities for the construction of calibration facilities with excellent performance and capabilities. This paper describes such a beamline, primarily built for the measurement of normal incidence multilayer mirrors in support of x-ray projection lithography programs.² However, its energy coverage, versatility, simplicity and convenience make it useful for a wide range of other experiments.

II. THE 6.3.2 BEAMLINE

Table I lists the relevant parameters of the optical components of the Calibration and Standards Beamline. Figure 1 is a schematic view of its installation at bending magnet port 6.3.2 at the ALS. The principal components are the following.

A. Four jaw aperture

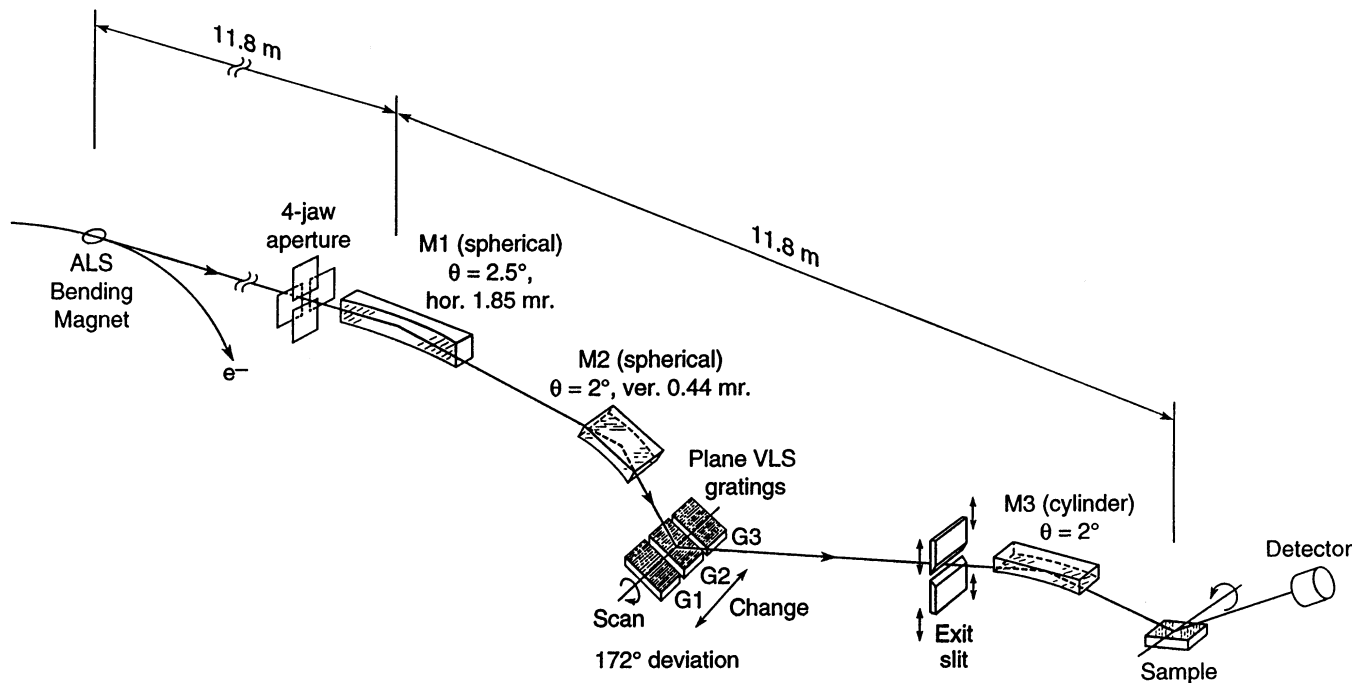
This consists of four cooled copper plates, each of which is mounted on a UHV feedthrough and can be inserted into the beam as far as required. This aperture is used to determine the horizontal and vertical acceptance of the beamline, up to the maximum of 1.85 mrad horizontally and 0.44 mrad vertically, determined by M1 and M2, respectively.

B. Horizontal focusing mirror (M1)

This mirror's function is to reimage the bending magnet source, horizontally and at unit magnification, on the sample at the center of the reflectometer chamber. It is made from single crystal silicon and is cooled by thermally contacting one side to a water-cooled stainless steel block, with a thin film of Ga-In eutectic interposed to ensure thermal contact. This simple side cooling method is very effective;

TABLE I. Optical components of ALS BL 6.3.2.

| Element | Distance (m) | | θ (deg) | Coating |
|-----------|--------------|--------------|-------------------------------|---------|
| | from source | Radius (m) | | |
| Aperture | 11.5 | - | - | - |
| M1 | 11.8 | 270.52 | 2.5 | Au/Ni |
| M2 | 16.0 | 83.36 | 2.0 | Au |
| Grating | 16.2 | ∞ | 172 (total included angle) | Au |
| Exit slit | 17.595 | - | - | - |
| M3 | 20.595 | 75- ∞ | 2.0 | Au |
| Sample | 23.595 | - | variable | - |



XBD 9509-04496.ILR

FIG. 1. Schematic of the layout of beamline 6.3.2 at the Advanced Light Source.

finite element analysis showed that the temperature rise of this mirror and the resultant distortion of the surface are negligible, even with ALS running at maximum power (400 mA at 1.9 GeV). The upper half of the mirror is coated with gold and the lower with nickel. Depending on the required energy coverage, either of these two coatings can be selected by translating the mirror laterally.

C. Monochromator

In a calibration and standards facility, accurate knowledge of the wavelength and reliability of the wavelength calibration are of prime importance. This requires a high resolution, high throughput monochromator that is simple and compact, with a stable geometry that can be accurately determined. These considerations led us to choose a monochromator of the type described by Hettrick and Underwood³ in which the mechanically ruled, plane VLS grating (VLS-PGM) operates in the converging light produced by a concave spherical mirror. In this version, the converging mirror M2 operates at a demagnification of 10:1. The large spherical aberration of the mirror used at high demagnification is corrected by adjusting the coefficients describing the variation of grating ruling. Optimization of these ruling parameters was carried out using the hybrid design method developed by Koike et al.,⁴ which takes advantage of the versatility of the ray-tracing method and the completeness of the analytical design method.⁵

The ALS design specifications called for minimal source motion: drifts of less than 1/10 of σ_x and σ_y during operation. Hence an entrance slitless design could be chosen.

Because this excellent source stability has been achieved in ALS operation, the slitless mode carries no penalty of drifts in wavelength calibration during scans. Wavelength shifts arising from source motions arising from changes in the storage ring operation parameters, for example, can be calibrated easily (see [e] below).

The present monochromator design has many practical advantages:

- Optimization of the grating line-space variation corrects all mirror M2 aberrations, allowing the monochromator to reach slit-width-limited resolution; in this case, the "slit" is the vertical source size of the ALS.
- The demagnification of the source allows a very short beamline, resulting in low cost and high mechanical stability. The increased vertical divergence allows better f-number matching for optics following the exit slit.
- Wavelength scanning is accomplished by rotation of the grating about its pole. No other motions, such as translation of the exit slit, are needed. This results in a very simple mechanical design.
- Entrance slitless operation allows maximal flux collection, simplifies the mechanical design and alignment, and further shortens the beamline.
- The zero order is focused at the exit slit (although it is not corrected for aberrations). This feature is extremely valuable for setup and alignment. It is possible to direct visible light from the storage ring through the exit slit to align optical components and the sample (see section F. below). The zero-order image can also be used to monitor vertical motions of the ALS source and thus to calibrate wavelength shifts.

- f) All optical surfaces required are either plane or spherical, simplifying fabrication and reducing cost.

The converging mirror was polished from single crystal silicon. Although provision was made for cooling this mirror by the same method as used for M1, this has not been found necessary. The monochromator has three interchangeable gratings having central groove densities of 300, 600 and 1200 l/mm, and the appropriate blaze angle. These were mechanically ruled on fused silica substrates. The grating sine bar is driven by a DC motor under the control of a closed-loop servo system, using a Heidenhain engraved glass scale with 0.1- μm divisions as a reference. A quadrature circuit divides each interval into 5 parts and positions the end of the sine bar within 20 nm. This allows, for example, a wavelength step size of 3 parts per million at 130 \AA .

D. Exit slit

The short exit arm of the monochromator results in a small linear dispersion at the exit slit, and hence exit slit widths of a few microns are required. Adjustments for position, parallelism and tilt are required to obtain the best performance. To meet these requirements, a mechanism was designed in which each of the four slit corners is independently actuated by a vacuum feedthrough and its position sensed to 0.1 μm by a capacitance micrometer. The range of slit widths that can be accommodated extend from zero to 400 μm .

E. Monochromator mechanical/vacuum design

The monochromator is designed to be very stable and to have precisely known geometry for absolute wavelength calibration via the known grating spacing. The optical components are mounted on three pedestals that mount to a baseplate *outside* the vacuum chamber (Figure 2). A flexible bellows surrounds each pedestal. These are prevented from collapsing under vacuum by flexural constraints that support the tank at the axis of each bellows. This scheme prevents the vacuum system from transmitting bending moments to the baseplate, ensuring stability against thermal drifts and

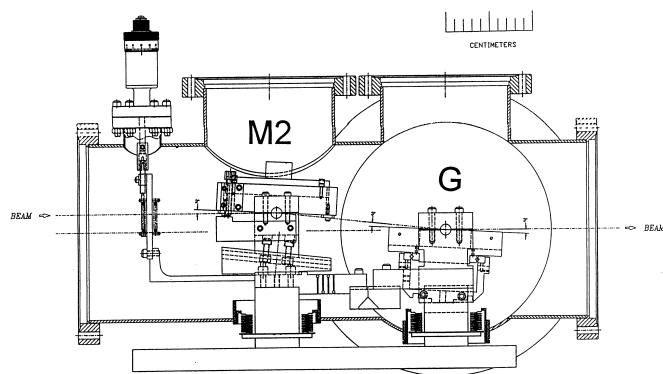


FIG. 2. Drawing of VLS-PGM monochromator.

vacuum loading distortions. All parts of the monochromator, to the exit slit, that contribute to the determination of the geometry are made of the same material (steel), and the monochromator is mounted on a single massive steel table. The internal components were first assembled outside of the vacuum chamber and their position determined using a measuring engine. They were then disassembled and reassembled in the vacuum chamber with a precision of a few μm . This procedure provided accurate knowledge of the optical geometry for absolute wavelength calibration.

F. Vertically refocusing mirror (M3)

The vertical refocusing mirror images the exit slit, at unit magnification, in the center of the reflectometer chamber. However, it is advantageous to be able to reimaging the slit elsewhere, such as in an auxiliary experimental chamber behind the reflectometer or at infinity to generate parallel light; this requires variable curvature. An unequal end couple mirror bender⁶ allows the mean radius of curvature of M3 to be varied and in addition provides a linear variation of the mirror radius and an image free from spherical aberration when M3 is used at other than unit magnification. M3 is an optical flat of uniform cross section polished from polycrystalline silicon.

III. EXPERIMENTAL FACILITIES

A. Reflectometer

The reflectometer is a two-axis vacuum goniometer using two Huber goniometers. One axis carries the sample, which may for example be a mirror at the center of the reflectometer vacuum tank (θ -motion). The other (ϕ -motion) carries the detector on a rotating arm. In addition there are through-vacuum linear motions to translate the sample in three orthogonal directions (x, y, z) with a position accuracy of 10 μm . All motions are controlled independently by computer. The sample itself is mounted on a kinematic holder that can be removed and replaced with high precision. The valve at the front of the reflectometer has a glass window; when closed, the sample can be positioned and aligned using visible synchrotron light, with the reflectometer at atmospheric pressure. Although the sample motions are primarily designed for measurement of optical components, they function as a sample manipulator with sufficient flexibility to allow a wide variety of different experiments to be carried out.

The reflectometer section is isolated from the monochromator by a differential ion pump, which can withstand 3 decades of pressure differential. Thus the sample chamber can be operated at pressures as high as 10^{-7} Torr with the beamline at 10^{-10} Torr. The reflectometer is equipped with a vibration-isolated cryopump having 4000 l/s pumping speed (for water vapor). This allows 1/2 hour pump down and turn around of samples.

B. Filter wheels and auxiliary experiments

The beamline contains two filter carousels, in which thin foils can be mounted to filter unwanted radiation or for the purpose of measuring their transmission. One of these is mounted upstream of the M3 mirror, the other just upstream of the reflectometer. A flange is provided at the back of the reflectometer for the attachment of additional experimental chambers, for which there is considerable floor space. The variable radius M3 mirror allows the beam to be vertically focused in this chamber.

C. Experiment control and data acquisition

The beamline and reflectometer are controlled by a Sun workstation through a VXI crate. The control and data analysis programs use LABVIEW™⁷ software. All monochromator and reflectometer functions (except sample changing) and data are controlled and displayed at the workstation, so that the beamline can be operated remotely. The software provides the capability of scanning monochromator wavelength λ or energy E, or scanning any of the reflectometer motions θ , ϕ , x , y , z , and for making special scans such as $\phi = 2\theta$, or 2-dimensional scans using any pair of motions.

IV. SELECTED RESULTS

The beamline has been installed, aligned, and operational since February 1995, and preliminary characterization of the flux, resolution, wavelength calibration, scattered light and higher order contamination has been carried out. To test the monochromator resolution, a gas absorption cell was used in the "auxiliary experiment" location. One benchmark of resolving power is the spectrum of the $1s-\pi^*$ vibrational states of molecular nitrogen. Figure 3 is a spectrum obtained using the 1200 l/mm grating. It is estimated that this

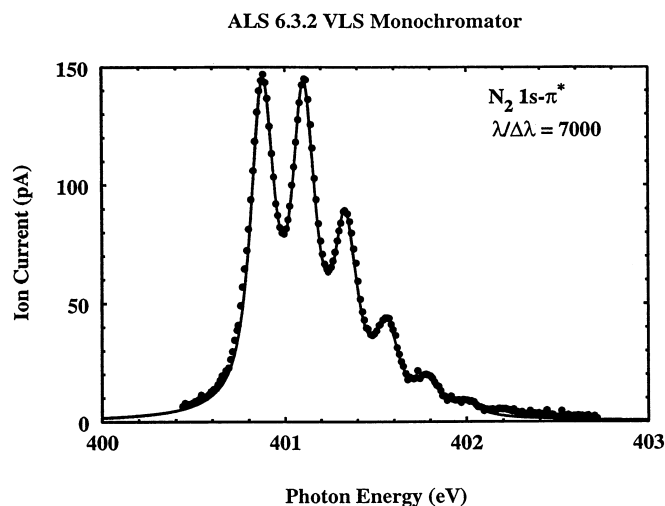


FIG. 3. Absorption spectrum at the $1s-\pi^*$ resonance of N_2 gas at 30 mTorr.

spectrum is obtained with the source size limited resolution of 7000.

Figure 4 is a reflectivity curve of a normal incidence multilayer mirror coated on a spherical surface. This mirror was tested for Lawrence Livermore National Laboratory's extreme UV projection lithography program. Although the signal to noise and the measurement precision are excellent, the measured reflectivity is a few percent less than that obtained using the laser-produced plasma reflectometer.¹ This is a result of higher order contamination. At present only filters are used to suppress higher orders; a more efficient order suppressor of a new design is being installed at the time of writing. It will be described in a forthcoming publication.

Figure 5 is an example of reflectivity measurements at higher energy, showing measurements of a W/BN multilayer mirror at a series of angles of incidence. The effect of the nitrogen absorption edge is clearly seen.

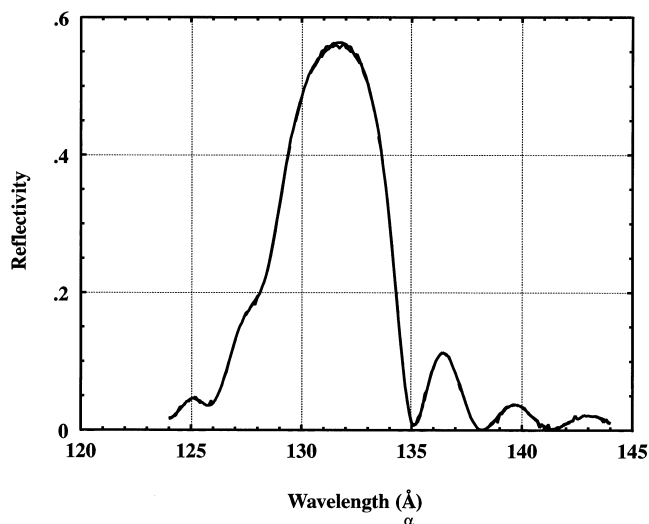


FIG. 4. Reflectivity vs λ of a normal incidence Mo-Si multilayer deposited on a spherical surface. The two curves represent separate measurements.

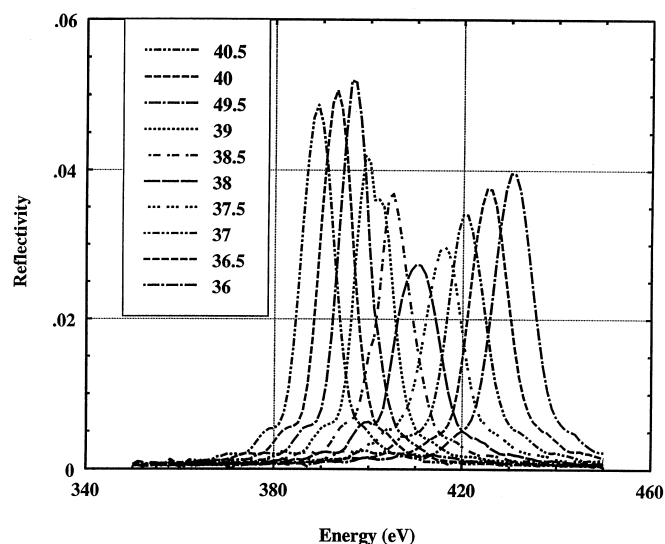


FIG. 5. Reflectivity vs. energy for a W/BN multilayer at various angles of glancing incidence, as shown in the box.

As an example of a different type of experiment, Figure 6 shows a series of B K x-ray absorption spectra of various boron compounds taken by the total electron yield method. The prominent sharp peaks at 191.8 and 193.8 eV exhibited by hBN and B₂O₃ have been attributed to very localized $p\pi^*$ states.⁸ It is seen that the B K absorption spectrum of B₄C prepared by sputtering is very different from that of the commercially obtained powder, indicating a possible stoichiometric change during sputtering. A more detailed description of these measurements is published elsewhere.⁹

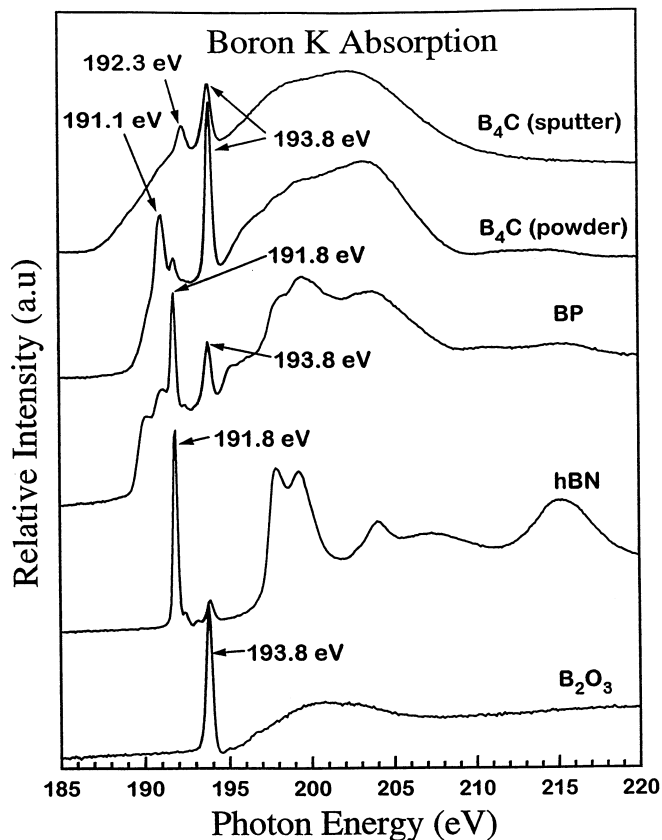


FIG. 6. B K-absorption spectra of various boron compounds obtained by total yield measurements.

ACKNOWLEDGMENTS

We are indebted to Dr. Kita of the Hitachi Corporation for the excellent work done in ruling the gratings and to Dr. R. C. C. Perera for help and encouragement. This work was supported by the Advanced Lithography Program of the Department of Defense Advanced Projects Research Agency, and the Director, Office of Energy Research, Office of Basic Energy Sciences, Materials Science U.S. Department of Energy, under contract number DE-AC03-76SF00098.

- ¹ E.M. Gullikson, J.H. Underwood, P.J. Batson, and V. Nikitin, *J. X-ray Sci. Tech.* **3**, 283 (1993).
- ² See, e.g., the special issue of *Applied Optics* (Vol. 32, No. 4, 1 December 1993) devoted to this topic.
- ³ M.C. Hettrick and J.H. Underwood, in *Short Wavelength Coherent Radiation: Generation and Applications*, edited by D.T. Attwood and J. Bokor, (AIP Conf. Proc. 147, 1986) p. 237; US Patent No. 4,776,696 (1988).
- ⁴ M. Koike, R. Beguristain, J.H. Underwood and T. Namioka, *Nucl. Inst. Meth. A* **347**, 273 (1994).
- ⁵ M. Koike and T. Namioka, *Appl. Opt.* **33**, 2048 (1994).
- ⁶ J.H. Underwood, *Space Sci. Instr.* **3**, 259 (1977).
- ⁷ LABVIEW™ is a trademark of National Instruments Corporation.
- ⁸ A. Chaiken, L.J. Terminello, J. Wong, G.L. Doll, and C.A. Taylor, *Appl. Phys. Lett.* **63**, 2112 (1993).
- ⁹ J. Jia, J.H. Underwood, E.M. Gullikson, T.A. Calcott, and R.C.C. Perera, *J. Electr. Spect. and Rel. Phenom.* (in press).